Prognostic and Therapeutic Impact of Argininosuccinate Synthetase 1 Control in Bladder Cancer as Monitored Longitudinally by PET Imaging

Michael D. Allen[1], Phuong Luong[1], Chantelle Hudson[1], Julius Leyton[1], Barbara Delage[1], Essam Ghazaly[1], Rosalind Cutts[1], Ming Yuan[1], Nelofer Syed[2], Cristiana Lo Nigro[9], Laura Lattanzio[9], Malgorzata Chmielewska-Kassassir[10], Ian Tomlinson[4], Rebecca Roylance[1,3], Hayley C. Whitaker[5], Anne Y. Warren[5], David Neal[5], Christian Frezza[6], Luis Beltran[3], Louise J. Jones[1,3], Claude Chelala[1], Bor-Wen Wu[11], John S. Bomalaski[11], Robert C. Jackson[7], Yong-Jie Lu[1], Tim Crook[8], Nicholas R. Lemoine[1], Stephen Mather[1], Julie Foster[1], Jane Sosabowski[1], Norbert Avril[1], Chien-Feng Li[12,13,14], and Peter W. Szlosarek[1,3]

Abstract

Targeted therapies have yet to have significant impact on the survival of patients with bladder cancer. In this study, we focused on the urea cycle enzyme argininosuccinate synthetase 1 (ASS1) as a therapeutic target in bladder cancer, based on our discovery of the prognostic and functional import of ASS1 in this setting. ASS1 expression status in bladder tumors from 183 Caucasian and 295 Asian patients was analyzed, along with its hypothesized prognostic impact and association with clinicopathologic features, including tumor size and invasion. Furthermore, the genetics, biology, and therapeutic implications of ASS1 loss were investigated in urothelial cancer cells. We detected ASS1 negativity in 40% of bladder cancers, in which multivariate analysis indicated worse disease-specific and metastasis-free survival. *ASS1* loss secondary to epigenetic silencing was accompanied by increased tumor cell proliferation and invasion, consistent with a tumor-suppressor role for *ASS1*. In developing a treatment approach, we identified a novel targeted antimetabolite strategy to exploit arginine deprivation with pegylated arginine deiminase (ADI-PEG20) as a therapeutic. ADI-PEG20 was synthetically lethal in *ASS1*-methylated bladder cells and its exposure was associated with a marked reduction in intracellular levels of thymidine, due to suppression of both uptake and *de novo* synthesis. We found that thymidine uptake correlated with thymidine kinase-1 protein levels and that thymidine levels were imageable with [^{18}F]-fluoro-L-thymidine (FLT)–positron emission tomography (PET). In contrast, inhibition of *de novo* synthesis was linked to decreased expression of thymidylate synthase and dihydrofolate reductase. Notably, inhibition of *de novo* synthesis was associated with potentiation of ADI-PEG20 activity by the antifolate drug pemetrexed. Taken together, our findings argue that arginine deprivation combined with antifolates warrants clinical investigation in ASS1-negative urothelial and related cancers, using FLT-PET as an early surrogate marker of response. *Cancer Res; 74(3); 896–907. ©2013 AACR.*

Introduction

Urothelial carcinoma is the fourth most common malignancy diagnosed in men, and the seventh commonest cause of solid cancer-related death in the United States, accounting for 15,000 deaths per annum (1). The 5-year overall survival rate of 40% to 60% for muscle invasive bladder cancer has plateaued over the past three decades, in part, due to the frequent comorbidities in this patient group (2). Moreover, despite $4.0 billion spent each year on bladder cancer treatment in the United States alone—one of the highest expenditures in

Authors' Affiliations: [1]Barts Cancer Institute—a Cancer Research UK Center of Excellence, John Vane Science Center, Queen Mary University of London; [2]Department of Medicine, Imperial College, Charing Cross Campus; [3]St Bartholomew's Hospital, Barts Health NHS Trust, West Smithfield, London; [4]Wellcome Trust Center for Human Genetics, Oxford; [5]Cancer Research UK Cambridge Research Institute, Li Ka Shing Center; [6]Hutchison/MRC Research Center, University of Cambridge, Medical Research Council Cancer Unit; [7]Pharmacometrics Ltd., Cambridge; [8]Dundee Cancer Center, University of Dundee, Ninewells Hospital, Dundee, United Kingdom; [9]Laboratory of Cancer Genetics and Translational Oncology, S Croce General Hospital, Cuneo, Italy; [10]Department of Structural Biology, Medical University of Lodz, Lodz, Poland; [11]Polaris Group, San Diego, California; [12]Department of Pathology, Chi-Mei Medical Center; [13]Department of Biotechnology, Southern Taiwan University of Science and Technology, Tainan, Taiwan; and [14]National Institute of Cancer Research, National Health Research Institutes, Tainan, Taiwan

Note: Supplementary data for this article are available at Cancer Research Online (http://cancerres.aacrjournals.org/).

M. Allen and P. Luong contributed equally as joint first authors and C.-F. Li and P.W. Szlosarek as joint last authors.

Corresponding Author: Peter W. Szlosarek, Center for Molecular Oncology, Barts Cancer Institute, Queen Mary University of London, Barts and The London School of Medicine and Dentistry, London EC1A 7BE, United Kingdom. Phone: 0044-207-882-3559; Fax: 0044-207-882-3884; E-mail: p.w.szlosarek@qmul.ac.uk

doi: 10.1158/0008-5472.CAN-13-1702

oncology—targeted therapies have been ineffective to date in this disease (3).

Recently, arginine auxotrophy or the absolute requirement for exogenous arginine for cellular growth has been detected in several chemoresistant solid cancers, including hepatocellular carcinoma, melanoma, mesothelioma, and prostate cancer (4–6). Arginine fuels an array of biosynthetic reactions, including proteins, nitric oxide (NO), polyamines, agmatine, and the amino acids proline and glutamate, and therefore may modulate tumorigenesis at multiple levels (7). Inactivation of the pleiotropic enzyme, argininosuccinate synthetase 1 (ASS1), with key roles in the urea cycle, citrulline–NO cycle, and arginine biosynthesis has emerged as a principal driver of tumoral arginine auxotrophy, with evidence for epigenetic silencing and hypoxia-inducible factor-1α (HIF-1α)–mediated transcriptional repression of *ASS1* (5, 8, 9). Significantly, ASS1 loss has been associated with decreased overall survival in ovarian cancer and myxofibrosarcoma, and reduced metastasis-free survival in osteosarcoma, implicating a tumor-suppressor function for this metabolic gene (10–12). Thus, arginine deprivation is being tested increasingly in the clinic, modeled on the successful introduction of another amino acid depletor, namely asparaginase, in the management of acute lymphoblastic leukemia five decades ago (13). Specifically, several early-phase trials of the arginine-degrading mycoplasmal enzyme, pegylated arginine deiminase (ADI-PEG20), have led to phase II/III randomized studies in melanoma, hepatocellular cancer, and mesothelioma (14–16).

Here, we characterized *ASS1* in bladder cancer based on the fact that loss of chromosome 9, including q34, the locus of *ASS1*, is a known early event in urothelial tumorigenesis (17). Previously, Linnenbach and colleagues provided evidence for a truncation mutation at the *ASS1* locus in a ureteric carcinoma sample, while searching for tumor suppressors at 9q34 (18). Here, we show that ASS1 negativity is a common event in bladder cancer detected in approximately 40% of tumors by immunohistochemistry (IHC). Furthermore, to address a putative tumor-suppressor role, we performed additional genetic and epigenetic studies of *ASS1* using a panel of bladder cancer cell lines. Finally, we studied the therapeutic consequences of ASS1 loss in bladder cancer, identifying a novel targeted antimetabolite strategy that combines arginine deprivation with the antifolate, pemetrexed. These studies were reinforced by metabolomic and positron emission tomography (PET) tracer analyses, which identify intracellular thymidine levels as a novel biomarker of early treatment response.

Materials and Methods

Primary tumor characteristics

Tissue microarrays (TMA) were constructed using a training set of biopsy samples, comprising 183 urothelial carcinomas collected at the Cancer Research UK Cambridge Research Institute (19), and an independent test set of 295 urothelial carcinomas, which were resected consecutively with curative intent in Chi Mei Medical Center, Taiwan, between January 1996 and March 2004. Institutional review boards in the United Kingdom (Cambridgeshire Local Research Ethics Committee) and Taiwan (IRB971006) ratified the tissue procurement. The diagnostic criteria were based on the updated American Joint Committee on Cancer Staging.

IHC

ASS1 IHC was performed using liver control sections as described previously (5). The scoring of thymidylate synthase (TS; 1:100, Clone EPR4545; Epitomics) and dihydrofolate reductase (DHFR;1:100, Clone EPR5285; Epitomics) was performed using an H-score, determined by the percentage and intensity of positively stained tumor cells with cases stratified according to high (no less than the median score) or low expression (less than the median score; ref. 20).

Cell lines and culture

Six bladder cancer cell lines were grown in a humidified atmosphere at 37°C and 5% CO_2 in endotoxin-free RPMI medium with 10% FBS (RT112, 5637, SCaBER, 253J, and T24) or Dulbecco's Modified Eagle Medium (DMEM) with 10% FBS (UMUC3). The arginine concentration was approximately 10-fold higher in the culture medium than found in human serum (i.e., 1 mmol/L vs. 0.06–0.1 mmol/L, respectively). Experiments were performed using cells at 70% confluency, which were harvested for analysis of *ASS1* promoter methylation, constitutive ASS1 mRNA, and protein. Studies of corroborative cell lines in a nonurothelial solid cancer (mesothelioma) were performed and all cell lines were authenticated by short tandem repeat profiling (LGC Standards).

Methylation-specific PCR

One microgram of genomic DNA was modified with sodium bisulphite using the EZ DNA methylation kit (Zymo) according to the manufacturer's instructions. Then, 50 ng of modified DNA was amplified using the following primers designed using the ASS1 promoter sequence: UF (5′ GTAGGAGGGAAGGGGTTTTT); UR (5′ ACAAAAAACAAATAACCCAAA); MF (5′ GTAGGAGGGAAGGGGTTTTC); and MR (5′ GCAAAAAACAAATAACCCGAA), in which U = unmethylated and M = methylated. Control CpGenome universal methylated and unmethylated DNA were obtained from Merck Millipore.

Pyrosequencing

Methylation in the -C-phosphate-G- (CpG) islands of the *ASS1* gene in the urothelial cell line panel was also analyzed using pyrosequencing technology. For pyrosequencing of the paraffin primary bladder cancer samples, PCR amplification and sequencing primers were optimized using the PyroMark Assay Design Software 2.0. Details of PCR primers and conditions are available on request.

Sequencing analysis

The coding exons and flanking sequences of ASS1 were analyzed by Sanger sequencing in forward and reverse in the panel of bladder cancer cell lines. Details of PCR primers and conditions are available on request.

Quantitative real-time reverse transcriptase PCR

Total RNA was extracted using the RNeasy Mini Kit (Qiagen) and reverse-transcribed with the High Capacity cDNA Reverse Transcription Kit (Applied Biosystems) according to the

manufacturer's instructions. Multiplex PCR was performed on an ABI Prism 7500 Real-Time PCR Instrument (Applied Biosystems). Primers and TaqMan probes for *ASS1* (FAM) and 18S (VIC) were obtained from Applied Biosystems (TaqMan Gene Expression Assays).

ASS1 overexpression and knockdown

ASS1 overexpression was performed in 253J, UMUC-3, and T24 bladder cancer cells using ASS1pIREShyg3 (or control) vector under hygromycin (200 μg/mL) selection, as described previously (10). ASS1 knockdown in 5637 bladder cancer cells was performed using the pSilencer 4.1-CMVpuro vector (Ambion) containing short hairpin RNA (shRNA) sequences targeting ASS1 (SMARTpool; Dharmacon) or a nontargeting control shRNA under puromycin (1 μg/mL) selection.

Proliferation assays

Briefly, 3×10^4 cells were suspended in 200 μL of serum-free DMEM, plated into a 96-well plate, and incubated for 48 hours. Subsequently, 40 μL of CellTitre Aqueous One solution (Promega, G3580) was added to each well and the plate was incubated for between 15 minutes to 1 hour before reading at 450 nm (Labtech, LT4000MS).

Invasion assays

Briefly, transwells (Corning, 3422) were coated with Matrigel (BD Bioscience, 354234) diluted 1:3 with serum-free DMEM and allowed to set for 1 hour at 37°C. Transwells were placed in the wells of a 24-well plate containing 500 μL of DMEM (PAA) with 10% serum. 3×10^4 cells in 200 μL of serum-free DMEM were plated into the top of the transwell, and incubated at 37°C for 48 hours. Transwells were removed from the DMEM + 10% FBS and placed into 500 μL of Trypsin/EDTA (PAA) for 1 hour at 37°C. The undersides of transwells were then washed with trypsin and the cell suspension transferred to 9.5 mL of Isoton and the number of cells quantified on a CASY counter. All experiments were repeated at least three times using quintuplicate readings.

Immunoblotting

Western blot analysis for ASS1 (BD Biosciences) was performed as described previously (5). Membranes were also probed for TS (Sigma-Aldrich), DHFR, TK1 (Abcam), p53R2 (Santa Cruz Biotechnology), PARP (Signal Transduction), β-actin, and Hsc70.

Drug treatments

Arginine depletion experiments were performed using ADI-PEG20 (Polaris Group) and 2% dialyzed FBS (>10 KDa, Autogen Bioclear). Cell viability was measured using the MTT assay according to manufacturer's instructions (Roche Diagnostics). Pemetrexed (Eli Lilly and Company) was purchased from Barts Chemopharmacy. Combination drug treatments of ADI-PEG20 and pemetrexed were studied using the Chou-Talalay methodology and the effect on tumor cell apoptosis was detected using PARP cleavage (Cell Signaling Technology) and Annexin V staining (21). Proteosome inhibition and demethylation experiments were performed using MG132 (1 μmol/L; Sigma-Aldrich) and 5-aza-2′-deoxycytidine (5-Aza-dC, 0.1–1 μmol/L; Sigma-Aldrich), respectively.

Liquid chromatography–mass spectrometry

PBS control and ADI-PEG20 treated cells (3×10^6) were washed twice with phosphate buffer saline and then harvested by adding 10 mL of ice-cold 80% methanol containing 0.1% formic acid (all reagents from Fisher Scientific). Cell extracts were prepared using a standard protocol and injected into the liquid chromatography–mass spectrometry (LC-MS) system. LC was performed using the nanoACQUITY UltraPerformance (UP) LC system (Waters) and MS was executed using a Waters Q-ToF Premier operated in positive and negative electrospray ionization modes. Data acquisition and analysis were performed using the Water Masslynx software (V 4.1) and MZmine software (version 2.2), respectively. Peak lists, including retention, M/Z, and peak intensities, were exported from MZmine and imported into Microsoft Office Excel 2007, revealing volcano plots and the fold change and *P* value for individual metabolites. Subsequent targeted metabolomic analysis was performed in the positive ion mode.

In vitro tracer uptake assays

Cells were plated at 1×10^5 cells per well the evening before the experiment. The next day cells were incubated with ADI-PEG20 (750 ng/mL). On the day of the assay, the drug media were removed and incubated in media supplemented with 2% dialyzed FBS for 1 hour. [^{3}H] thymidine was then added at 1 μci/mL to each well and incubated for a further 1 hour. Cells were then washed twice in ice-cold PBS, and harvested with trypsin. The cell lysates were collected and added to tubes containing 2 mL of scintillation fluid and the cell-associated ^{3}H radioactivity was measured using the β scintillation counter (LKB Instruments). The radioactivity uptake in nmoles was normalized to the number of viable cells to give pmole uptake per 10,000 live cells and expressed relative to untreated controls. All experiments were done in triplicate and repeated 3 times.

In vivo experiments

UMUC-3 cells (1×10^7 in 0.1 mL) were implanted into the flank of CD1 nu/nu mice and developed into visible tumors by 11 days. For the *in vivo* [^{18}F]-fluoro-L-thymidine (FLT)–PET studies, animals ($n = 5$) were injected i.v. via the tail vein with 15 to 18 MBq of [^{18}F]-FLT and imaged using an Inveon microPET/CT (Siemens) before and 24 hours after treatment with ADI-PEG20 (5 IU). Standardized uptake values (SUV) were calculated by dividing the activity concentration in each voxel by the injected dose and dividing by the animal weight. For drug combination studies, mice were separated into four intraperitoneal (i.p.) treatment groups ($n = 11$ per group): PBS control (days 1 and 8), ADI-PEG20 (5 IU on days 1 and 8), pemetrexed (PEM; 100 mg/kg on days 2–4 and 9–11); and ADI-PEG20 (5 IU on days 1 and 8) plus PEM (100 mg/kg on days 2–4 and 9–11). Tumor volume and animal weights were recorded and all mice were sacrificed on day 11; tumors were collected and stored for immunohistochemical analyses. Additional ^{18}F-FLT microPET/CT imaging was performed in female UMUC3 bladder cancer

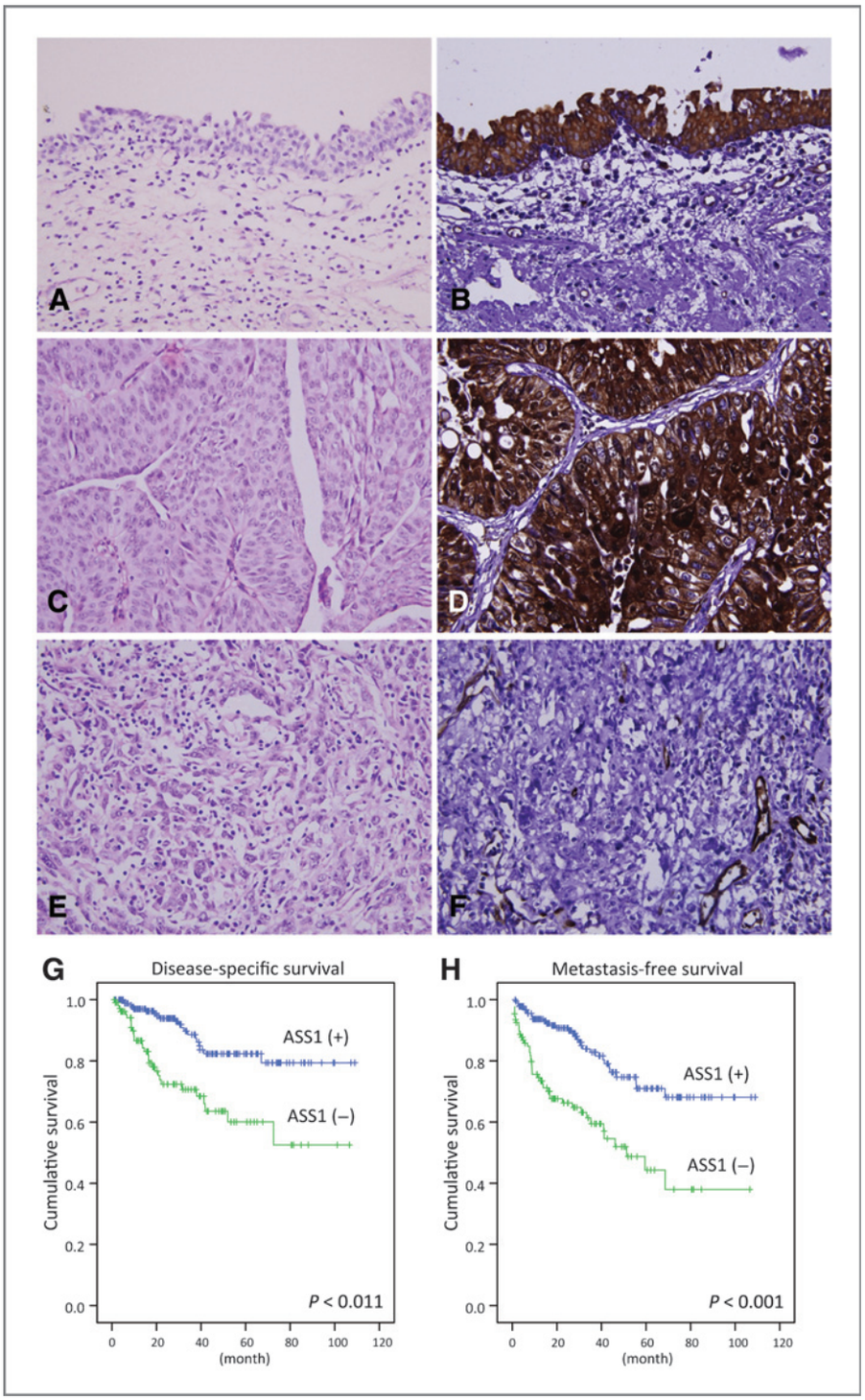

Figure 1. ASS1 IHC and clinical correlation in bladder cancer. Representative hematoxylin and eosin and ASS1 staining of normal urothelium (A and B), low-grade (C and D), and high-grade (E and F) urothelial carcinomas (X400). ASS1 expression is present in normal urothelium and the low-grade lesion but absent in the high-grade lesion, with vascular endothelial cells serving as the positive internal control. ASS1 deficiency is highly predictive of worse disease-specific (G) and metastasis-free survival (H) by log-rank tests.

tumor-bearing CD1 nude mice ($n = 5$ per group) assessing the drug combination. Animals were imaged at baseline immediately before i.p. treatment with 5 IU ADI (ADI and PEM + ADI treatment groups) or PBS (PBS and PEM treatment groups) and imaged again 24 hours later. Immediately after the 24-hour imaging timepoint, the PEM and PEM + ADI treatment groups received 100 mg/kg PEM i.p. for 5 days whereas the others received PBS, with ^{18}F-FLT imaging carried out on day 7.

Statistical analysis

GraphPad Prism version 5.0 and SPSS 14.0 were used to test results for statistical significance. The associations of ASS1

Table 1. Multivariate analysis for disease-specific and metastasis-free survival in bladder cancer

		DSS			MeFS		
Parameter	**Category**	**HR**	**95% CI**	***P* value**	**HR**	**95% CI**	***P* value**
Primary tumor (T)	Ta	1	—	<0.001[a]	1	—	0.003[a]
	T1	3.546	1.60–7.874		5.965	1.671–21.301	
	T2-4	28.571	3.07–250.00		7.821	2.169–28.200	
Mitotic activity (10 HPF)	<10	1	—	0.009[a]	1	—	0.004[a]
	> = 10	2.451	1.248–4.817		2.143	1.269–3.619	
ASS1 expression	Positive	1	—	0.011[a]	1	—	0.001[a]
	Deficient	2.233	1.201–4.153		2.336	1.419–3.847	
Nodal status (N)	N0	1	—	0.994	1	—	0.257
	N1-2	1.003	0.463–2.175		1.446	0.764–2.737	
Perineural invasion	Absent	1	—	0.160	1	—	0.120
	Present	1.974	0.764–5.105		1.815	0.856–3.850	
Vascular invasion	Absent	1	—	0.481	1	—	0.957
	Present	1.299	0.373–1.592		1.017	0.553–1.872	
Histologic grade	Low grade	1	—	0.944	1	—	0.696
	High grade	1.058	0.192–4.641		1.238	0.425–3.607	

Abbreviations: CI, confidence interval; DSS, disease-specific survival; MeFS, metastasis-free survival.
[a]Statistically significant.

expression level with clinicopathologic factors were evaluated using the χ^2, Fisher exact, or Wilcoxon rank-sum test as appropriate. For all analyses, two-sided tests of significance were used with $P < 0.05$ considered significant.

Results

Loss of ASS1 confers poor survival in bladder cancer

First, we screened for ASS1 expression in a training set bladder cancer TMA derived from a European population revealing that 45% (83 of 183) of biopsies were ASS1-negative. The validation TMA (Fig. 1A–F) from an Asian population yielded similar results with 37% of bladder cancer cases (108 of 295) being ASS1-negative. ASS1 negativity conferred a poor disease-specific ($P = 0.011$) and metastasis-free survival ($P = 0.001$) on multivariate analysis (Fig. 1G and H and Table 1). Furthermore, ASS1 loss was linked to several adverse clinicopathologic features, including increased tumor size and grade, lymph node involvement, and vascular invasion (Supplementary Tables S1 and S2).

Methylated *ASS1* is linked to increased proliferation and invasion of bladder cancer cells

To understand the regulation of ASS1 expression and its role in urothelial malignancy, we screened six bladder carcinoma cell lines for genomic and epigenetic alterations. FISH analysis confirmed all lines were either triploid or tetraploid with the *ASS1* locus intact (data not shown). There were no mutations in *ASS1* and no loss of heterozygosity in the region immediately surrounding *ASS1* (data not shown). Instead, the UMUC-3 and 253J cell lines were fully methylated, whereas the T24 line was partially methylated at the *ASS1* promoter, with negligible *ASS1* mRNA and no ASS1 protein. In contrast, all the *ASS1*-unmethylated cell lines (SCaBER, RT112, and 5637) expressed ASS1 mRNA and protein (Fig. 2A). Notably, *ASS1* promoter methylation was greatest in UMUC-3 and 253J compared with the T24 cell line by pyrosequencing of six CpG islands within the *ASS1* promoter. In contrast, the ASS1-positive bladder cancer cell lines were unmethylated by pyrosequencing validating the results obtained with MS-PCR (Fig. 2B). The demethylating agent decitabine reexpressed ASS1 protein in 253J, UMUC-3, and T24 cells, confirming epigenetic silencing as a key mechanism involved in *ASS1* inactivation in bladder cancer cells (data not shown; ref. 22).

To determine the correlation between immunohistochemical expression of ASS1 and methylation status, tissue blocks of an independent set of 30 urothelial carcinomas with a high tumor cell content (>70%) were selected for pyrosequencing. Following optimization of primers for paraffin-embedded tissue, only one ASS1-positive tumor had an average methylation value of 45% that was greater than the threshold value of 40% (Supplementary Fig. S1). The remaining tumors with methylation values >40% were all negative for ASS1 immunoexpression ($P < 0.001$), validating the role of promoter methylation in *ASS1* silencing in primary bladder cancer (Supplementary Table S3).

Next, we addressed the significance of epigenetic loss of *ASS1* in bladder cancer by manipulating *ASS1* in our panel of urothelial cancer cell lines. Although *ASS1* overexpression decreased the proliferation of 253J and UMUC-3 cells, *ASS1* siRNA increased the proliferation of 5637 cells, consistent with a tumor-suppressor role for *ASS1* in urothelium (Fig. 2C). We also observed a reciprocal relationship between *ASS1* expression and cell invasion by performing matrigel invasion assays, confirming that *ASS1* loss increased the invasiveness of urothelial tumor cells *in vitro* (Fig. 2D).

ASS1-methylated bladder cancer cell lines are sensitive to ADI-PEG20

To test the effect of arginine deprivation on bladder cancer cell line viability, we treated the panel of bladder cancer cell lines with the arginine depletor, ADI-PEG20. All ASS1-negative

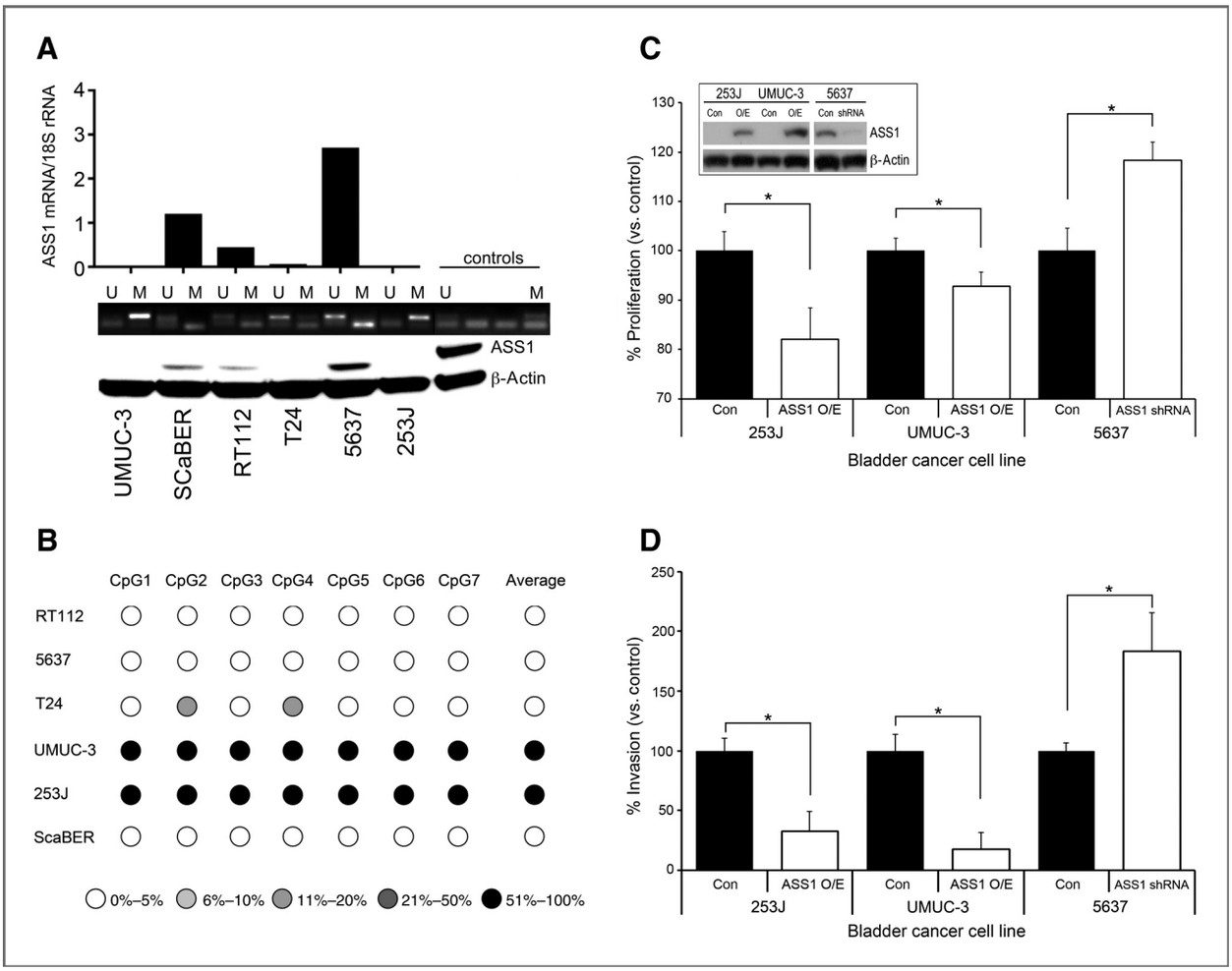

Figure 2. Epigenetic silencing of *ASS1* in bladder cancer linked to increased tumor cell proliferation and invasion. A, *ASS1* mRNA, protein, and methylation status of a panel of six bladder cancer cell lines. B, pyrosequencing revealed more *ASS1* methylation in 253J and UMUC-3 cells than T24 cells, whereas 5637, SCaBER, and RT112 cells were unmethylated, consistent with the MS-PCR data. C, overexpressing (O/E; inset) *ASS1* in UMUC-3 and 253J cell lines resulted in a significant (5%–20%) reduction in proliferation, respectively; in contrast, knockdown of endogenous ASS1 (inset) in 5637 cells caused a significant 20% increase in proliferation. *, $P < 0.0001$ (three independent experiments). D, overexpression of *ASS1* in 253J and UMUC-3 cell lines caused a significant (50% and 75%, respectively) reduction of invasion, whereas knockdown of endogenous *ASS1* in 5637 cells resulted in a significant (75%) increase in invasion. *, $P < 0.0001$ (three independent experiments). Con, control empty vector cells.

cell lines were sensitive to ADI-PEG20 with the highly methylated lines 253J and UMUC-3 displaying the greatest sensitivity to arginine depletion; in contrast, the ASS1-positive cell lines 5637, RT112, and SCaBER were resistant to ADI-PEG20 (Fig. 3A). Moreover, forced *ASS1* overexpression in ASS1-negative cell lines reduced their sensitivity to ADI-PEG20, validating the role of *ASS1* loss in mediating the synthetic lethal effect to arginine deprivation (Fig. 3B).

ADI-PEG20 inhibits pyrimidine metabolism in *ASS1*-negative tumor cells

We proceeded to analyze the metabolic effects of ADI-PEG20 and confirmed a significant decrease in intracellular arginine with a corresponding increase in citrulline in ASS1-negative bladder cancer cells. Marked reductions in thymidine and increases in thymine and glutamine were also detected by LC/MS (Fig. 4A). In contrast, ADI-PEG20 reduced arginine levels to a minor extent in the ASS1-positive RT112 control cell line, whereas intracellular levels of thymidine, thymine, and glutamine were unaffected, indicating a nonessential role for exogenous arginine. Because of these differential effects on intracellular thymidine, we interrogated gene pathways modulated by ADI-PEG20, identifying downregulation of the folate-dependent nucleotide synthesizing enzymes TS and DHFR specifically in ASS1-negative tumor cells (data not shown). Marked suppression of DHFR and TS mRNA and protein was detected in all three ADI-sensitive bladder cancer cell lines whereas no effect was seen in the RT112 control cell line exposed to ADI-PEG20 (Fig. 4B and C). We also analyzed the thymidine salvage pathway, as a compensatory source of cellular thymidine upon suppression of *de novo* pyrimidine synthesis. Unexpectedly, ADI-PEG20 also reduced ^{3}H-thymidine uptake in the arginine-auxotrophic cell

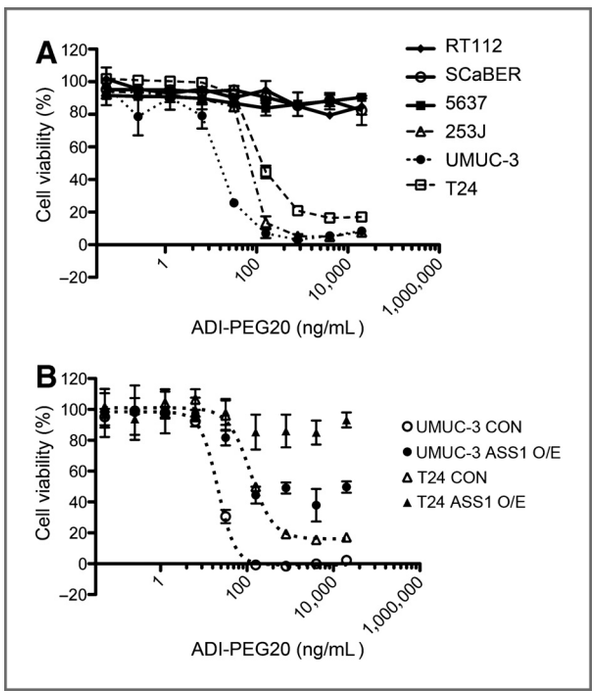

Figure 3. ADI-PEG20 is cytotoxic to *ASS1*-methylated bladder cancer cell lines. A, bladder cancer cell line viability following exposure to varying doses of ADI-PEG20 (0–20,000 ng/mL) was assessed by MTT assay at 6 days. B, overexpression of ASS1 in *ASS1*-methylated cell lines induced resistance to ADI-PEG20 by 6 days of ADI-PEG20 treatment, most marked in the T24 cell line, validating ASS1 loss as a biomarker of sensitivity to arginine deprivation.

lines associated with downregulation of thymidine kinase 1 (TK1; ref. 23), with no effect in RT112 control cells (Fig. 4D and E). Notably, cotreatment with MG132, a proteosome inhibitor that blocks protein degradation, abrogated the ADI-PEG20–induced suppression of TS and TK1 levels (Fig. 4F). More generally, similar data on thymidine salvage and *de novo* synthesis pathways were obtained in a panel of ADI-treated ASS1-negative (methylated) mesothelioma cell lines (Supplementary Fig. S2). Finally, we assessed whether *in vivo* imaging of thymidine uptake could provide an early biomarker of response to ADI-PEG20 therapy using UMUC-3 xenografts. Consistent with our *in vitro* studies, there was a 66% decrease in the maximum standardized uptake value (SUVmax) on [^{18}F]FLT-PET after 24 hours of ADI-PEG20 therapy (Fig. 4G).

Enhanced effect of ADI-PEG20 and pemetrexed in bladder cancer

To exploit our findings in the clinic, we used the multitargeted antifolate pemetrexed, which blocks enzymes, including TS and DHFR, and is reported to have modest activity in bladder cancer (24). High TS expression, in particular, has been linked to poor clinical outcome and resistance to antifolates in cancers of the bladder, lung, mesothelium, and colon (25–29). Moreover, bladder TMA analysis revealed that ASS1 loss was associated with a reciprocal increase in TS and DHFR expression—both linked to poor outcome for disease-specific and metastasis-free survival—emphasizing the interdependence between arginine auxotrophy and modulation of nucleotide biosynthesis (Supplementary Fig. S3 and S4; and Supplementary Table S1). Thus, we hypothesized that ADI-PEG20 may potentiate the cytotoxicity of pemetrexed in ASS1-negative tumor cells via modulation of folate-dependent enzymes. First, we showed that pemetrexed and ADI-PEG20 enhanced apoptosis compared with either agent alone by increasing PARP cleavage and Annexin V binding *in vitro* in *ASS1*-methylated tumor cell lines (Fig. 5A and B). Secondly, ADI-PEG20 significantly reduced tumor growth of the UMUC-3 cell line ($P < 0.001$) in xenografted nude mice. Although pemetrexed alone had no effect, the combination was more effective than ADI-PEG20 alone ($P < 0.05$; Fig. 5C and D). Analysis of tumors from the xenograft studies confirmed reduced TS, DHFR, and TK1 levels in ADI-PEG20–treated animals (Fig. 5E). Finally, to validate our results we executed an [^{18}F]-FLT microPET/CT imaging study of the combination therapy in the UMUC-3 xenograft tumor model. Our SUVmax data showing the superior efficacy of the ADI-PEG20 and pemetrexed drug combination over that of ADI-PEG20 alone are consistent with our earlier tumor volumetric measurements (Fig. 5F). Notably, there was a lack of effect on SUVmax of pemetrexed in animals that had not been pretreated with ADI-PEG20.

Discussion

Progress in the targeted therapy of advanced urothelial carcinoma has lagged behind other urological malignancies, especially prostate and renal cancer. For the first time, we have identified *ASS1* as a novel bladder cancer biomarker with wider implications for the therapy and monitoring of cancers dependent on exogenous arginine for survival. We show that despite exhibiting a poorer prognosis, ASS1-negative bladder cancer is amenable to dual targeting with ADI-PEG20 and antifolates with early treatment response monitoring by [^{18}F]FLT-PET.

Our bladder cancer cell line studies reveal that unmethylated *ASS1* functions as a *bona fide* tumor suppressor and is consistent with recent studies in osteosarcomas and myxofibrosarcomas (11, 12). Exactly how *ASS1* promoter methylation leads to a requirement for exogenous arginine, which promotes increased tumor cell proliferation and invasion is unclear. Interestingly, previous studies have associated exogenous arginine with DNA synthesis in Burkitt lymphoma cells and with increased proliferation of caco-2 colon cancer cells via a glutamine-dependent effect (30, 31). Yamauchi and colleagues proposed that under conditions of limited arginine supply intracellular glutamine is diverted for arginine synthesis as supplying exogenous arginine was shown to promote nucleotide synthesis. We found for the first time that upon depletion of arginine in ASS1-negative tumor cells, glutamine levels increased indicative of a block on nucleotide synthesis. Thus, our metabolomic experiments with ADI-PEG20 support the hypothesis that the *ASS1* epimutation reprograms extracellular arginine so that it is sparing for glutamine in nucleotide metabolism. Additional metabolomic flux studies are under way to explore further the interdependence of arginine and glutamine in the context of tumoral ASS1-deficiency. Exogenous arginine has also been shown to stimulate intestinal cell

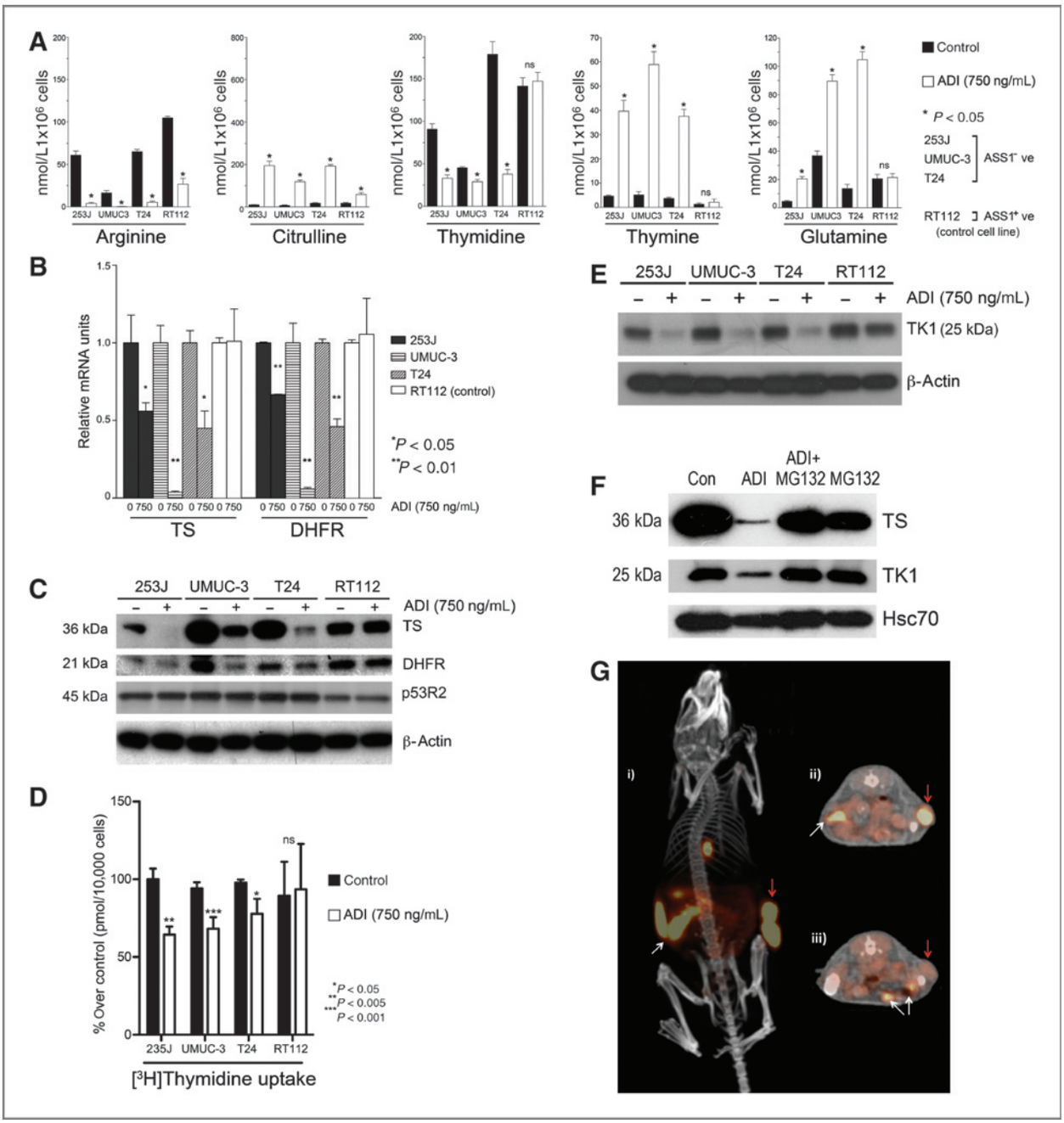

Figure 4. ADI-PEG20 modulates pyrimidine metabolism in *ASS1*-methyated cancer cells. A, cell extracts from ASS1-negative bladder cancer lines and the RT112 control treated with ADI-PEG20 (750 ng/mL) for 24 hours were subjected to metabolomic analysis by LC/MS. Arginine decreased in all cell lines; however, the reduction was at least 1-log fold greater in the ASS1-negative tumor cells. Glutamine and thymine increased whereas thymidine decreased specifically in the ADI-treated ASS1-negative bladder cell lines with no effect in RT112 control cells. Data, mean and SE ($n = 6$). ADI-PEG20 downregulated TS and DHFR mRNA (B) and protein (C) by 24 hours specifically in the *ASS1*-methylated cell lines. In contrast, the DNA synthetic enzyme ribonucleotide reductase subunit p53R2 was unaltered, confirming the specific downregulatory effect of ADI-PEG20 on TS and DHFR proteins; β-actin was used as the loading control (50). D, [^{3}H]thymidine uptake in bladder cancer cells after treatment with ADI-PEG20 (750 ng/mL). The cells remaining after ADI treatment decreased their uptake of thymidine by 24 hours in all ASS1-negative cell lines except the T24 bladder cell line, which showed a reduction by 72 hours (*, $P < 0.05$; **, $P < 0.005$). In contrast, [^{3}H] thymidine uptake was unchanged in the control RT112 cell line after ADI treatment. Data, mean and SE ($n = 9$). E, ADI-PEG20 reduced TK1 protein levels by 24 hours specifically in ASS1-negative bladder cancer cell lines. β-actin was used as the loading control. F, ADI-PEG20–mediated loss of TS and TK1 can be abrogated by inhibiting the proteasome with MG132. UMUC-3 cells were plated and incubated overnight; subsequently, cells were exposed to DMSO (Con), ADI-PEG20 (750 ng/mL), ADI-PEG20, and MG132 or MG132 (1 μmol/L) for 24 hours with immunoblotting as shown. G, [^{18}F]-FLT microPET/CT imaging in a UMUC-3 bladder tumor-bearing CD1 nude mouse (i) before treatment showing uptake in tumor (red arrow), and increased tracer concentration in intestine (white arrow) and also gall bladder. Transverse views before (ii) and 24 hours after (iii) treatment with 5 IU ADI-PEG20 show a reduction in tumor SUVmax after treatment (3.2 vs. 1.1 after treatment), indicating a decrease in tumor cell proliferation.

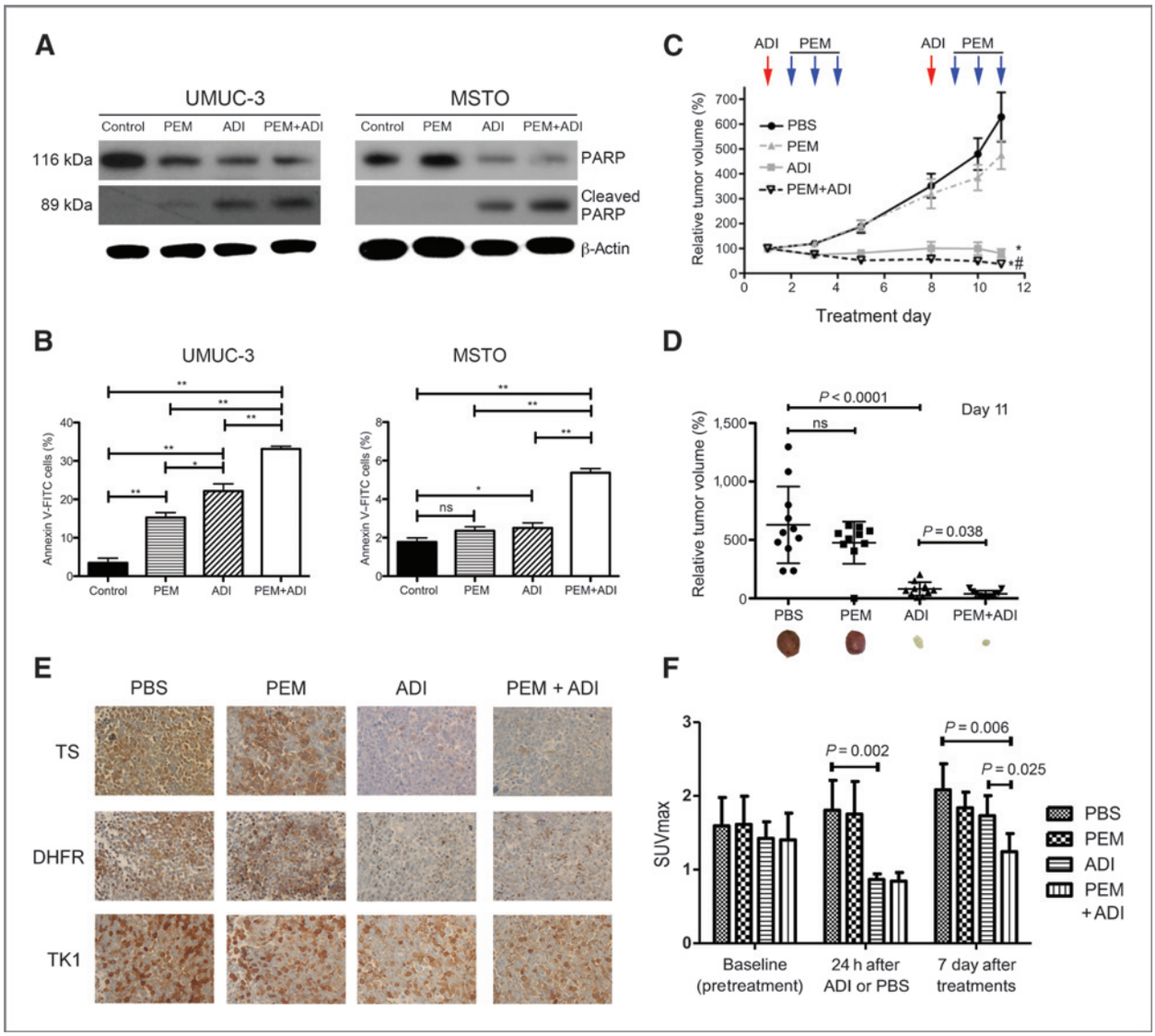

Figure 5. ADI-PEG20 sensitizes *ASS1*-methylated cancer cells to pemetrexed. ASS1-negative bladder cancer cells (UMUC-3) and malignant mesothelioma cells (MSTO) were treated with fixed doses of ADI-PEG20 and pemetrexed (PEM; Supplementary Table S4) with enhanced cell killing *in vitro* and *in vivo*: increased PARP cleavage by Western blotting (A) and increased Annexin V (B) staining by FACS were observed in the combination drug treatment compared with either drug alone by 96 hours ($n = 6$). C and D, xenograft experiment showing enhanced control of UMUC-3 cells with the combination compared with either drug alone (#, $P < 0.05$). ADI-PEG20, but not pemetrexed, had significant single agent activity compared with vehicle control (*, $P < 0.001$). E, representative TS, DHFR, and TK1 IHC (X400) showing reduced expression of all three enzymes in ADI-treated UMUC-3 xenograft tumors; residual strong DHFR staining in stromal cells compared with negative tumor cells with ADI-PEG20 treatment. Pemetrexed and ADI-PEG20 treatments reduce and relocate TK1 expression from the nucleus to the cytoplasm; the drug combination further reduces TK1 expression compared with either drug alone. F, [^{18}F]-FLT microPET/CT imaging response to treatment of ASS1-negative UMUC-3 tumors to ADI-PEG20 combined with pemetrexed. The ADI-treated animals showed a decrease in [^{18}F]-FLT SUVmax compared with PBS as seen previously ($P < 0.05$; Fig. 4G). Imaging at 7 days showed a significant decrease in SUVmax for the PEM + ADI treatment group vs. PBS control ($P < 0.01$) as well as PEM + ADI vs. ADI alone ($P < 0.05$).

motility via activation of NO and focal adhesion kinase signaling (32, 33). In particular, arginine is a dominant amino acid modulator of mTOR, a nodal pathway that integrates cell growth, proliferation, invasion, and metastasis of various cancers, including urothelial malignancy (34–36); moreover, arginine deprivation has been shown to repress mTOR and its downstream substrates p70 S6 kinase and 4E-BP1 in ASS1-negative cancer cells (6, 37). Indeed, it is becoming clear that arginine deprivation has multiple effects on gene expression and that this is likely to be determined not only by cell type but also by the status of the *ASS1* gene (38).

The ADI-PEG20–induced suppression of the folate-dependent enzymes TS and DHFR and sensitization of ASS1-negative tumor cells to the cytotoxic effects of pemetrexed provide a novel metabolic approach to retargeting cytotoxic chemotherapy (39). Our results also validate the work of Cheng and

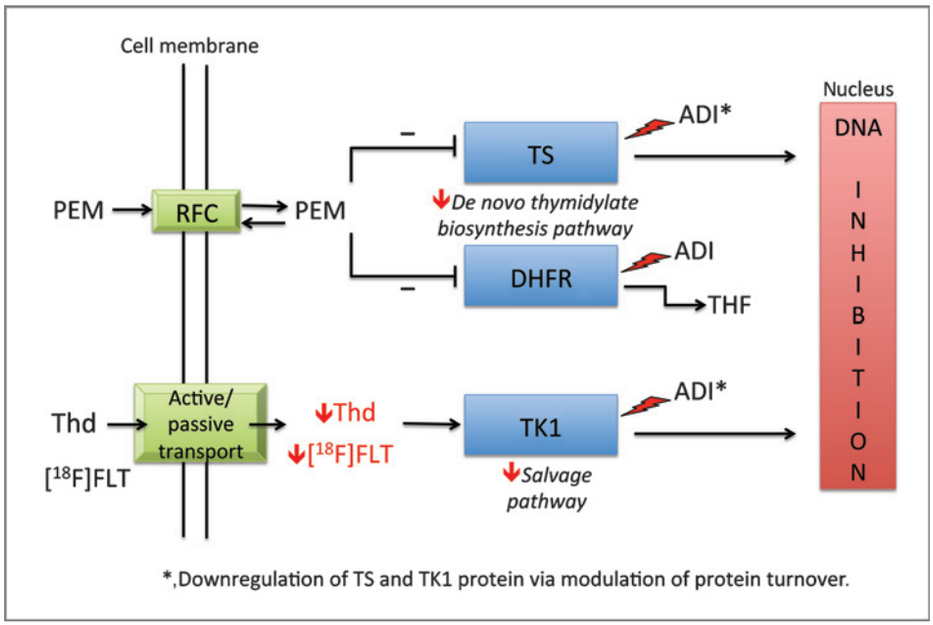

Figure 6. Schematic of the inhibitory effects of ADI-PEG20 on *de novo* thymidylate biosynthesis and salvage pathways in bladder cancer. ADI-PEG20 suppresses TS and DHFR protein and sensitizes ASS1-negative bladder cancer cells to the cytotoxic effects of pemetrexed. In addition, ADI-PEG20 blocks thymidine uptake linked to reduced TK1 protein, which is detectable using [^{18}F]FLT-PET. RFC, reduced folate carrier; THF, tetrahydrofolate.

colleagues, who showed that the irreversible TS inhibitor 5-fluorouracil was more effective when combined with pegylated human arginase in a hepatocellular carcinoma xenograft (40). It is noteworthy that the ADI-PEG20 and antifolate doublet has a wide therapeutic window in the xenograft studies. Moreover, our experience from an ongoing clinical trial of arginine depletion in mesothelioma (NCT01279967) includes a patient treated concurrently with ADI-PEG20 and the antifolate methotrexate for an unrelated condition; the combination was safe and led to a prolonged period of disease control (manuscript in preparation) (51).

Furthermore, the decreased uptake of thymidine following ADI-PEG20 treatment as shown by the ^{3}H-thymidine and FLT tracer studies may be exploited as an early therapeutic biomarker for imaging *ASS1*-methylated tumors. This is in contrast to recent work with ADI-PEG20 in ASS1-negative melanoma xenografts in which there was no effect on TK1 expression and FLT-PET metabolic responses were not detected (41). These and previous results using 2[^{18}F]fluoro-2-deoxy-D-glucose tracers may be explained in part by the differential regulation of *ASS1* promoter with HIF-1α–mediated repression in melanoma compared with epigenetic silencing identified in several other arginine auxotrophic cancers (9, 16, 42).

Thus, arginine deprivation with ADI-PEG20 suppresses both the *de novo* and salvage pathways of nucleotide synthesis in ASS1-negative bladder cancer cells, which may be exploited for therapy and imaging, respectively (Fig. 6). In addition to ADI-PEG20 modulating protein turnover as indicated by the MG132-mediated recovery of TS and TK1 enzymes, several other mechanisms may underlie the reduced levels of target proteins, including chemical attack by peroxynitrite, a potent oxidant and nitrating species generated by arginine deprivation (43–45). More generally, the reciprocal relationship between thymidine and glutamine in ASS1-negative tumors reinforces several other preclinical approaches targeting amino acid utilization in cancer, including methionine, glycine, and serine (46–49). Significantly, we observed that ASS1 downregulation was linked to the reciprocal upregulation of the serine biosynthetic pathway enzymes, PHGDH, PSAT1, and PSPH, in bladder cancer (data not shown), and this warrants further evaluation in view of the important roles of serine in tumor cell proliferation and bioenergetics.

In conclusion, our studies linking the biology of arginine auxotrophic bladder cancer to adverse clinicopathologic variables accentuate ASS1 loss as a novel biomarker for evaluation in patients with urothelial cancer. Specifically, targeted modulation of pyrimidine synthesis—via suppression of the *de novo* and salvage nucleotide pathways—using arginine-depleting drugs combined with antifolates has the potential to improve the management of urothelial and related cancers with methylated *ASS1*.

Disclosure of Potential Conflicts of Interest

J.S. Bomalaski is executive VP Medical Affairs with Polaris Pharmaceuticals, Inc. R.C. Jackson is a consultant and advisory board member of Polaris Inc. N.R. Lemoine is the editor of Gene Therapy journal (self employed with honorarium paid by publisher) with Nature Publishing Group. No potential conflicts of interest were disclosed by the other authors.

Authors' Contributions

Conception and design: Y.-J. Lu, T. Crook, C.-F. Li, P.W. Szlosarek
Development of methodology: M. Allen, P. Luong, C. Hudson, E. Ghazaly, L. Lattanzio, D. Neal, C. Frezza, L.J. Jones, T. Crook, S. Mather, J. Sosabowski, N. Avril, P.W. Szlosarek
Acquisition of data (provided animals, acquired and managed patients, provided facilities, etc.): M. Allen, P. Luong, J. Leyton, E. Ghazaly, M. Yuan, N. Syed, I. Tomlinson, R. Roylance, H.C. Whitaker, A.Y. Warren, L.J. Jones, N.R. Lemoine, S. Mather, J. Foster, J. Sosabowski, N. Avril, P.W. Szlosarek
Analysis and interpretation of data (e.g., statistical analysis, biostatistics, computational analysis): P. Luong, C. Hudson, J. Leyton, E. Ghazaly, R. Cutts, H.C. Whitaker, C. Frezza, L. Beltran, L.J. Jones, C. Chelala, J.S. Bomalaski, R.C. Jackson, Y.-J. Lu, T. Crook, S. Mather, J. Foster, J. Sosabowski, N. Avril, C.-F. Li, P.W. Szlosarek
Writing, review, and/or revision of the manuscript: M. Allen, J. Leyton, E. Ghazaly, R. Roylance, H.C. Whitaker, J.S. Bomalaski, Y.-J. Lu, T. Crook, S. Mather, J. Sosabowski, N. Avril, C.-F. Li, P.W. Szlosarek

Administrative, technical, or material support (i.e., reporting or organizing data, constructing databases): P. Luong, B. Delage, M. Chmielewska-Kassassir, B.-W. Wu, Y.-J. Lu, C.-F. Li, P.W. Szlosarek
Study supervision: C. Lo Nigro, N.R. Lemoine, S. Mather, J. Sosabowski, C.-F. Li, P.W. Szlosarek

Acknowledgments

The authors thank Melissa Phillips, Patricia Gorman, Kimberly Howarth, and Duncan Jodrell for technical assistance, and Daniel Berney, Jeremy Steele, Simon Joel, Lucyna Wozniak, Marco Merlano, and Simon Pacey for additional administrative support.

Grant Support

This work was funded by a Cancer Research UK Clinician Scientist Fellowship (Dr. P.W. Szlosarek; C12522/A8632) and by Barts and The London Charity.

The costs of publication of this article were defrayed in part by the payment of page charges. This article must therefore be hereby marked *advertisement* in accordance with 18 U.S.C. Section 1734 solely to indicate this fact.

Received June 17, 2013; revised October 29, 2013; accepted November 3, 2013; published OnlineFirst November 27, 2013.

References

1. Mitra AP, Datar RH, Cote RJ. Molecular pathways in invasive bladder cancer: new insights into mechanisms, progression, and target identification. J Clin Oncol 2006;24:5552–64.
2. Sonpavde G, Watson D, Tourtellott M, Cowey CL, Hellerstedt B, Hutson TE, et al. Administration of cisplatin-based chemotherapy for advanced urothelial carcinoma in the community. Clin Genitourin Cancer 2012;10:1–5.
3. Dovedi SJ, Davies BR. Emerging targeted therapies for bladder cancer: a disease waiting for a drug. Cancer Metastasis Rev 2009;28:355–67.
4. Ensor CM, Holtsberg FW, Bomalaski JS, Clark MA. Pegylated arginine deiminase (ADI-SS PEG20,000 mw) inhibits human melanomas and hepatocellular carcinomas in vitro and in vivo. Cancer Res 2002;62:5443–50.
5. Szlosarek PW, Klabatsa A, Pallaska A, Sheaff M, Smith P, Crook T, et al. In vivo loss of expression of argininosuccinate synthetase in malignant pleural mesothelioma is a biomarker for susceptibility to arginine depletion. Clin Cancer Res 2006;12:7126–31.
6. Kim RH, Coates JM, Bowles TL, McNerney GP, Sutcliffe J, Jung JU, et al. Arginine deiminase as a novel therapy for prostate cancer induces autophagy and caspase-independent apoptosis. Cancer Res 2009;69:700–8.
7. Delage B, Fennell DA, Nicholson L, McNeish I, Lemoine NR, Crook T, et al. Arginine deprivation and argininosuccinate synthetase expression in the treatment of cancer. Int J Cancer 2010;126:2762–72.
8. Husson A, Brasse-Lagnel C, Fairand A, Renouf S, Lavoinne A. Argininosuccinate synthetase from the urea cycle to the citrulline-NO cycle. Eur J Biochem 2003;270:1887–99.
9. Tsai WB, Aiba I, Lee SY, Feun L, Savaraj N, Kuo MT. Resistance to arginine deiminase treatment in melanoma cells is associated with induced argininosuccinate synthetase expression involving c-Myc/HIF-1alpha/Sp4. Mol Cancer Ther 2009;8:3223–33.
10. Nicholson LJ, Smith PR, Hiller L, Szlosarek PW, Kimberley C, Sehouli J, et al. Epigenetic silencing of argininosuccinate synthetase confers resistance to platinum-induced cell death but collateral sensitivity to arginine auxotrophy in ovarian cancer. Int J Cancer 2009;125:1454–63.
11. Kobayashi E, Masuda M, Nakayama R, Ichikawa H, Satow R, Shitashige M, et al. Reduced argininosuccinate synthetase is a predictive biomarker for the development of pulmonary metastasis in patients with osteosarcoma. Mol Cancer Ther 2010;9:535–44.
12. Huang HY, Wu WR, Wang YH, Wang JW, Fang FM, Tsai JW, et al. ASS1 as a novel tumor suppressor gene in myxofibrosarcomas: aberrant loss via epigenetic DNA methylation confers aggressive phenotypes, negative prognostic impact, and therapeutic relevance. Clin Cancer Res 2013;19:2861–72.
13. Old LJ, Boyse EA, Campbell HA, Daria GM. Leukaemia-inhibiting properties and L-asparaginase activity of sera from certain South American rodents. Nature 1963;198:801.
14. Ascierto PA, Scala S, Castello G, Daponte A, Simeone E, Ottaiano A, et al. Pegylated arginine deiminase treatment of patients with metastatic melanoma: results from phase I and II studies. J Clin Oncol 2005;23:7660–8.
15. Glazer ES, Piccirillo M, Albino V, Di Giacomo R, Palaia R, Mastro AA, et al. Phase II study of pegylated arginine deiminase for nonresectable and metastatic hepatocellular carcinoma. J Clin Oncol 2010;28:2220–6.
16. Szlosarek PW, Luong P, Phillips MM, Baccarini M, Ellis S, Szyszko T, et al. Metabolic response to pegylated arginine deiminase in mesothelioma with promoter methylation of argininosuccinate synthetase. J Clin Oncol 2013;31:e111–3.
17. Miyao N, Tsai YC, Lerner SP, Olumi AF, Spruck CH 3rd, Gonzalez-Zulueta M, et al. Role of chromosome 9 in human bladder cancer. Cancer Res 1993;53:4066–70.
18. Linnenbach AJ, Robbins SL, Seng BA, Tomaszewski JE, Pressler LB, Malkowicz SB. Urothelial carcinogenesis. Nature 1994;367:419–20.
19. Veerakumarasivam A, Goldstein LD, Saeb-Parsy K, Scott HE, Warren A, Thorne NP, et al. AURKA overexpression accompanies dysregulation of DNA-damage response genes in invasive urothelial cell carcinoma. Cell Cycle 2008;7:3525–33.
20. Budwit-Novotny DA, McCarty KS, Cox EB, Soper JT, Mutch DG, Creasman WT, et al. Immunohistochemical analyses of estrogen receptor in endometrial adenocarcinoma using a monoclonal antibody. Cancer Res 1986;46:5419–25.
21. Chou TC. Drug combination studies and their synergy quantification using the Chou-Talalay method. Cancer Res 2010;70:440–6.
22. Delage B, Luong P, Maharaj L, O'Riain C, Syed N, Crook T, et al. Promoter methylation of argininosuccinate synthetase-1 sensitises lymphomas to arginine deiminase treatment, autophagy and caspase-dependent apoptosis. Cell Death Dis 2012;3:e342.
23. Brockenbrough JS, Souquet T, Morihara JK, Stern JE, Hawes SE, Rasey JS, et al. Tumor 3′-deoxy-3′-(18)F-fluorothymidine ((18)F-FLT) uptake by PET correlates with thymidine kinase 1 expression: static and kinetic analysis of (18)F-FLT PET studies in lung tumors. J Nucl Med 2011;52:1181–8.
24. Galsky MD, Mironov S, Iasonos A, Scattergood J, Boyle MG, Bajorin DF. Phase II trial of pemetrexed as second-line therapy in patients with metastatic urothelial carcinoma. Invest New Drugs 2007;25:265–70.
25. Li Y, Li X, Dai H, Sun X, Li J, Yang F, et al. Thymidylate synthase was associated with patient prognosis and the response to adjuvant therapy in bladder cancer. BJU Int 2009;103:547–52.
26. Takezawa K, Okamoto I, Okamoto W, Takeda M, Sakai K, Tsukioka S, et al. Thymidylate synthase as a determinant of pemetrexed sensitivity in non-small cell lung cancer. Br J Cancer 2011;104:1594–601.
27. Righi L, Papotti MG, Ceppi P, Bille A, Bacillo E, Molinaro L, et al. Thymidylate synthase but not excision repair cross-complementation group 1 tumor expression predicts outcome in patients with malignant pleural mesothelioma treated with pemetrexed-based chemotherapy. J Clin Oncol 2010;28:1534–9.
28. Sigmond J, Backus HH, Wouters D, Temmink OH, Jansen G, Peters GJ. Induction of resistance to the multitargeted antifolate Pemetrexed (ALIMTA) in WiDr human colon cancer cells is associated with thymidylate synthase overexpression. Biochem Pharmacol 2003;66:431–8.
29. Edler D, Kressner U, Ragnhammar P, Johnston PG, Magnusson I, Glimelius B, et al. Immunohistochemically detected thymidylate synthase in colorectal cancer: an independent prognostic factor of survival. Clin Cancer Res 2000;6:488–92.
30. Osunkoya BO, Adler WH, Smith RT. Effect of arginine deficiency on synthesis of DNA and immunoglobulin receptor of Burkitt lymphoma cells. Nature 1970;227:398–9.
31. Yamauchi K, Komatsu T, Kulkarni AD, Ohmori Y, Minami H, Ushiyama Y, et al. Glutamine and arginine affect Caco-2 cell proliferation by promotion of nucleotide synthesis. Nutrition 2002;18:329–33.

32. Rhoads JM, Chen W, Gookin J, Wu GY, Fu Q, Blikslager AT, et al. Arginine stimulates intestinal cell migration through a focal adhesion kinase dependent mechanism. Gut 2004;53:514–22.
33. Rhoads JM, Liu Y, Niu X, Surendran S, Wu G. Arginine stimulates cdx2-transformed intestinal epithelial cell migration via a mechanism requiring both nitric oxide and phosphorylation of p70 S6 kinase. J Nutr 2008;138:1652–7.
34. Hara K, Yonezawa K, Weng QP, Kozlowski MT, Belham C, Avruch J. Amino acid sufficiency and mTOR regulate p70 S6 kinase and eIF-4E BP1 through a common effector mechanism. J Biol Chem 1998;273:14484–94.
35. Hansel DE, Platt E, Orloff M, Harwalker J, Sethu S, Hicks JL, et al. Mammalian target of rapamycin (mTOR) regulates cellular proliferation and tumor growth in urothelial carcinoma. Am J Pathol 2010;176:3062–72.
36. Laplante M, Sabatini DM. mTOR signaling in growth control and disease. Cell 2012;149:274–93.
37. Savaraj N, You M, Wu C, Wangpaichitr M, Kuo MT, Feun LG. Arginine deprivation, autophagy, apoptosis (AAA) for the treatment of melanoma. Curr Mol Med 2010;10:405–12.
38. Brasse-Lagnel CG, Lavoinne AM, Husson AS. Amino acid regulation of mammalian gene expression in the intestine. Biochimie 2010;92:729–35.
39. Vander Heiden MG. Targeting cancer metabolism: a therapeutic window opens. Nat Rev Drug Discov 2011;10:671–84.
40. Cheng PN, Lam TL, Lam WM, Tsui SM, Cheng AW, Lo WH, et al. Pegylated recombinant human arginase (rhArg-peg5,000mw) inhibits the in vitro and in vivo proliferation of human hepatocellular carcinoma through arginine depletion. Cancer Res 2007;67:309–17.
41. Stelter L, Fuchs S, Jungbluth AA, Ritter G, Longo VA, Zanzonico P, et al. Evaluation of arginine deiminase treatment in melanoma xenografts using F-FLT PET. Mol Imaging Biol 2013;15:768–75.
42. Stelter L, Evans MJ, Jungbluth AA, Zanzonico P, Ritter G, Ku T, et al. Novel mechanistic insights into arginine deiminase pharmacology suggest 18F-FDG is not suitable to evaluate clinical response in melanoma. J Nucl Med 2012;53:281–6.
43. Morrow K, Hernandez CP, Raber P, Del Valle L, Wilk AM, Majumdar S, et al. Anti-leukemic mechanisms of pegylated arginase I in acute lymphoblastic T-cell leukemia. Leukemia 2013;27:569–77.
44. Dabrowska-Mas E, Fraczyk T, Ruman T, Radziszewska K, Wilk P, Ciesla J, et al. Tyrosine nitration affects thymidylate synthase properties. Org Biomol Chem 2012;10:323–31.
45. Noris M, Todeschini M, Cassis P, Pasta F, Cappellini A, Bonazzola S, et al. L-arginine depletion in preeclampsia orients nitric oxide synthase toward oxidant species. Hypertension 2004;43:614–22.
46. Kokkinakis DM, Liu X, Chada S, Ahmed MM, Shareef MM, Singha UK, et al. Modulation of gene expression in human central nervous system tumors under methionine deprivation-induced stress. Cancer Res 2004;64:7513–25.
47. Zhang WC, Shyh-Chang N, Yang H, Rai A, Umashankar S, Ma S, et al. Glycine decarboxylase activity drives non-small cell lung cancer tumor-initiating cells and tumorigenesis. Cell 2012;148:259–72.
48. Jain M, Nilsson R, Sharma S, Madhusudhan N, Kitami T, Souza AL, et al. Metabolite profiling identifies a key role for glycine in rapid cancer cell proliferation. Science 2012;336:1040–4.
49. Possemato R, Marks KM, Shaul YD, Pacold ME, Kim D, Birsoy K, et al. Functional genomics reveal that the serine synthesis pathway is essential in breast cancer. Nature 2011;476:346–50.
50. Yamaguchi T, Matsuda K, Sagiya Y, Iwadate M, Fujino MA, Nakamura Y, et al. p53R2-dependent pathway for DNA synthesis in a p53-regulated cell cycle checkpoint. Cancer Res 2001;61:8256–62.
51. Szlosarek PW, Steele JP, Sheaff MT, Avril NE, Szyszko T, Ellis S, et al. A randomised phase II trial of pegylated arginine deiminase (ADI-PEG20) in patients with malignant pleural mesothelioma (MPM). In: 2013 World Conference on Lung Cancer; 2013 Oct 27-30; Sydney. Abstr no. MO09.02.